High rejection, tunable parallel resonance in micromachined lead zirconate titanate on silicon resonators

Sarah S. Bedair,[1,a)] Daniel Judy,[1] Jeffrey Pulskamp,[1] Ronald G. Polcawich,[1] Adam Gillon,[1] Eugene Hwang,[2] and Sunil Bhave[2]
[1]*U.S. Army Research Laboratory, Adelphi, Maryland 20783, USA*
[2]*OxideMEMS Laboratory, Cornell University, Ithaca, New York 14853, USA*

(Received 10 June 2011; accepted 19 August 2011; published online 9 September 2011)

This paper presents a micromachined lead zirconate titanate-on-silicon electromechanical resonator, tunable from series to parallel resonance, for either bandstop or bandpass filter applications. Scattering parameter measurements (9.2 V direct current (DC) bias) reveal bandstop rejection levels > 109 dB at 59.74 MHz and passband loss of 40 dB with a −20-dB bandwidth of 25 kHz (0.042%). These compare within 5-dB of the models. Parallel resonance is also observed for an alternate mechanical mode at 182.8 MHz with a 1.5 V DC bias with a rejection of 54.7 dB, a −20 dB bandwidth of 41 kHz (0.022%). This mode is tunable with the electric field to show series resonance. © *2011 American Institute of Physics*. [doi:10.1063/1.3636432]

Communication systems motivate the need for high quality factor resonators and filters with low loss and power consumption. Tunable filters can significantly reduce the size of multiband, analog front-end systems. There has been prior work in radio frequency microelectromechanical system (RF-MEMS) mechanical resonators for bandpass filter applications[1–3] and alternate applications such as miniature power converters.[4] Piezoelectric MEMS (PiezoMEMS) mechanical resonators show promise for high levels of integration and performance across a wide frequency range (MHz to GHz).[5–7] In addition, tunable bandstop filters are of interest for interference signal suppression. Examples of bandstop filters include tunable absorptive notch filters[8] and RF-MEMS capacitive switches and gallium arsenide varactors with a 24-dB rejection and a 0.8-dB passband loss at 10 GHz.[9]

This work advances prior thin-film lead zirconate titanate (PZT) resonator work,[10] where improved series resonance motional resistance and quality factor were demonstrated using PZT-on-silicon versus PZT-only resonators. This paper presents the use of RF-MEMS electromechanical resonators as high rejection, parallel resonators, which can be used in bandstop applications. The existence of high rejection, parallel resonances is proven, through experiments and circuit models, to be a consequence of the cancellation of motional and feed-through currents. Analog tuning, through electric field biasing of the ferroelectric PZT, enables one to tailor the feed-through current to precisely cancel the motional current, thereby, achieving high rejection. The key advance in this work is threefold: (1) the combination of passive circuit elements with PiezoMEMS resonators to achieve high rejection (>109 dB) parallel resonance, (2) the development of theory predicting the DC bias conditions for series versus parallel resonance, and (3) the frequency response tuning of either parallel or series resonance on a single device.

Two fabricated device types are under consideration (Fig. 1). Figure 1(a) illustrates a device similar to that previously published.[11] For the second device type (type-II), illustrated in Fig. 1(b), the PZT and the bottom platinum (Pt) electrode common to the drive and sense port are removed for isolation. The general circuit model of the type-I resonator including the routing parasitics is illustrated in Fig. 1(c). The frequency dependent impedances are $Z_r(s)$, the motional impedance of the resonator, $Z_d(s)$, the impedance of the drive capacitance, $Z_s(s)$, the impedance of the sense capacitance, $Z_g(s)$, the impedance to ground, $Z_A(s)$, the source, and $Z_L(s)$ is the load impedance. The complex variable, s, is represented by $j\omega$, where ω is the frequency. Assuming $Z_r(s) \gg Z_L(s)$ and $\frac{i_g(s)}{i_f(s)} \approx \frac{Z_s(s)+Z_L(s)}{Z_g(s)}$, the motional, $i_r(s)$, to feed-through, $i_f(s)$, current ratio is

$$\frac{i_r(s)}{i_f(s)} = \frac{Z_s(s)}{Z_r(s)}\left(\frac{Z_d(s)}{Z_s(s)}\left(1+\frac{i_g(s)}{i_f(s)}\right)+1\right) \approx \frac{1}{Z_r(s)}\left(Z_d(s)\left(1+\frac{Z_s(s)+Z_L(s)}{Z_g(s)}\right)+1\right). \quad (1)$$

Unity magnitude and ± 180° phase for Eq. (1) result in the cancellation of the motional and feed-through current, which leads to high rejection, parallel resonance. For the type-II device, the ratio, $i_r(s)/i_f(s)$, is much greater than unity in the frequency range of interest.

The device fabrication is similar to that described by Ref. 11. The length, L_{elec}; width, w_{elec}, of both devices' top electrodes (Fig. 1(b)); and gap in the PZT and platinum, w_{gap}, are 196, 14, and 4 μm, respectively. The device length, L_{tot}, and width, w_{tot}, are 200 and 40 μm, respectively. The Pt thickness is 100 nm, the device silicon is 10 μm, and the PZT is 0.5 μm.

To assess the validity of Eq. (1), possible candidates for high rejection, parallel modes were identified in the high feed-through, type-I devices by assessing the motional parameters of the identical modes in the high isolation, type-II devices. The frequency response of the type-II resonator revealed a mode with a series motional resistance equivalent to the impedance satisfying the parallel resonance condition as described in Eq. (1) at ~59.6 MHz. This frequency

a)Author to whom correspondence should be addressed. Electronic mail: sarahbedair@gmail.com..

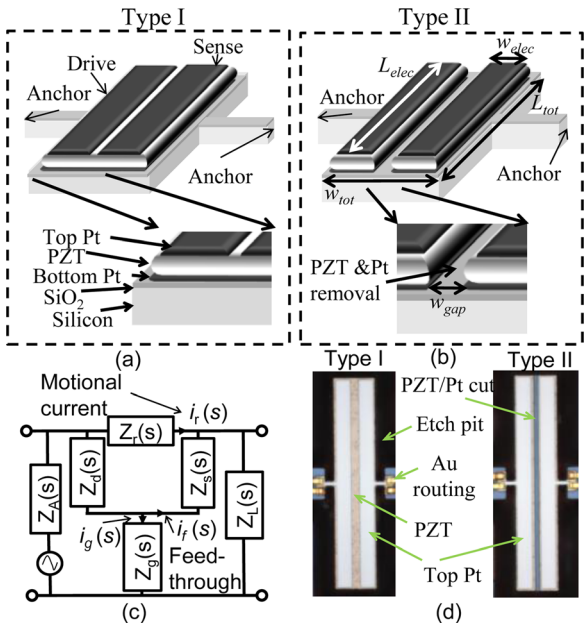

FIG. 1. (Color online) Illustrations of the two fabricated device types: (a) type-I without and (b) type-II with removed PZT and common Pt electrode. (c) Equivalent circuit of the type-I device with source and load impedances and labeled motional current, $i_r(s)$, due to the electromechanical resonator and feed-through current, $i_f(s)$. (d) Top view of the fabricated devices.

response is shown in Fig. 2(a), where a dc bias is superimposed to the alternating current signal at both input and output ports using bias-tees. The motional resistances (and series resonance quality factor, Q_{ser}) at 5, 10, and 15 V DC bias conditions were extracted to be 4600 Ω ($Q_{ser} = 370$), 5130 Ω ($Q_{ser} = 370$), and 6080 Ω ($Q_{ser} = 460$), respectively. The bias dependent motional resistances for this mode satisfy the parallel resonance condition for the type-I resonator in contrast to the series resonance measured for the type-II resonator. In other words, the type-II series resonance magnitude of −35.6 dB (10-V bias) is similar to the −36.5 dB feed-through for the type-I case under similar bias conditions. The bias dependent frequency response for the type-I resonator case, with $Z_g = 1.7$ Ω, is shown in Fig. 2(b). The measured response reveals parallel resonance with high attenuation and covers a tuning range of 59.65 to 59.78 MHz over 3 to 14 V DC bias. The measured insertion loss (9.2 V) at 59.5 MHz is 36.2 dB, with a 109-dB rejection at 59.74 MHz, and a −20-dB bandwidth of 25 kHz (0.042%).

The scattering parameters of the electrical circuit representing the type-I device were modeled using two-port network theory. The measured parallel resonance rejection versus bias voltage is compared to the model where both the dielectric constant and the effective piezoelectric stress constant, e_{31_eff}, DC bias dependence are scaled accordingly.[12] Note, the dielectric constant and e_{31_eff} parameters are extracted from capacitive and displacement test structures, respectively, at low frequencies versus the electric field. The model and experimental results for the parallel resonance rejection (Fig. 3(a)) compare well and are within 5 dB of each other. The minimum parallel resonance magnitude, −109 dB at 9.2 V, is at the noise floor of the measurement instrument while the theoretical minimum magnitude is −113 dB. The sharpness of the parallel resonance frequency response, S_{par}, versus bias voltage is extracted and compared to the model in Fig. 3(b). This is defined by the following:

$$S_{par} = \frac{f_{\min}}{\Delta f_{3dB}}, \tag{2}$$

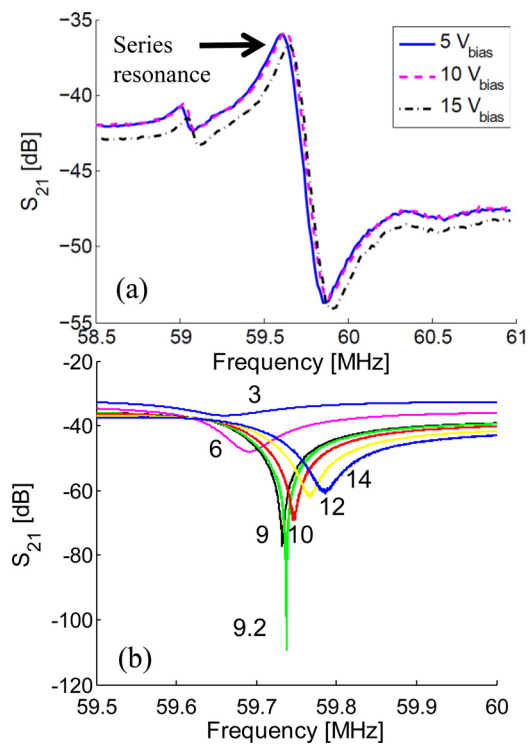

FIG. 2. (Color online) (a) Forward transmission coefficient, S_{21}, of the type-II, high isolation and (b) type-I devices under varying DC bias conditions (V_{bias}) on both the input and output ports.

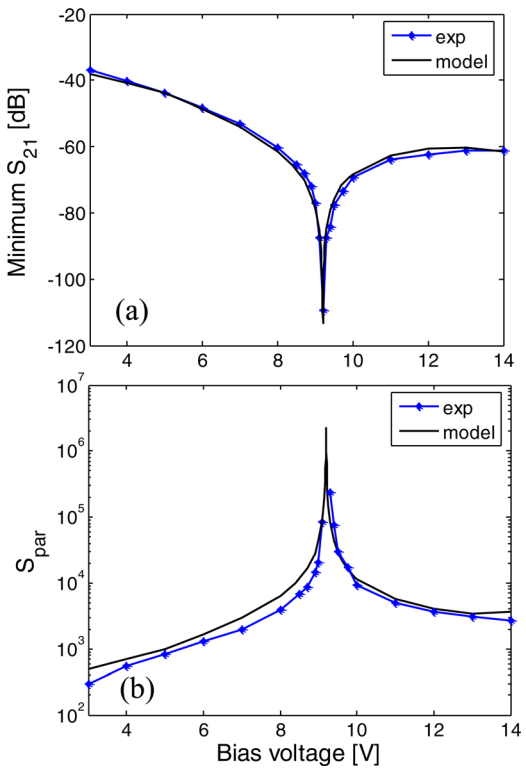

FIG. 3. (Color online) (a) The modeled and extracted minimum S_{21} from Fig. 2(b) and (b) the associated sharpness of the parallel resonance frequency response as defined by Eq. (2).

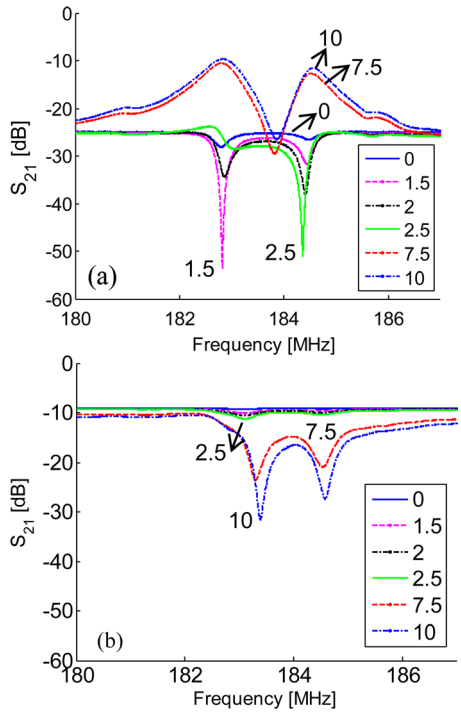

FIG. 4. (Color online) The frequency response of the type-I higher order modes with (a) $Z_g = 1.65\ \Omega$ and (b) $Z_g = 15\ \Omega$ revealing the impact of the finite resistance to ground on the response.

where f_{min} is the frequency at the minimum S_{21} magnitude and Δf_{3dB} is the width at double the magnitude at f_{min}. Although S_{par} was not extracted for the 9.2-V case, the maximum theoretical S_{par} is 2.2×10^6. It is important to note that high S_{par} does not represent mechanical quality factor as this process is associated with current cancellation and not directly with energy dissipation.

There are conditions for which the bias voltage can be leveraged to tune for either a parallel or series resonance frequency response. Through a similar process as described previously, this condition was predicted for two higher frequency modes at 182.8 and 184.6 MHz. The measured responses (type-I device) for varying bias conditions are shown in Fig. 4(a). For the 182.8-MHz mode, parallel resonance is observed at 1.5 V with a 54.7-dB rejection and a 41 kHz (0.022%) at a −20-dB bandwidth. The passband insertion loss is 25 dB at 180 MHz. For the same mode, series resonance is observed by tuning the bias voltage at both ports to higher voltages (7.5 and 10 V). Similar tuning behavior is observed for the 184.6-MHz mode.

An identical type-I device was designed with a larger Z_g resistance of 15 Ω. This value was chosen to assess the sensitivity of the parallel to series tuning to higher resistances to ground and, hence, higher feed-through. The measured response is shown in Fig. 4(b). In contrast to Fig. 4(a), a parallel to series change in the frequency response is not observed with a similar DC bias range. The feed-through signal is much larger than the motional signal with the 0–2.5 V DC bias range. Parallel resonance is observed (10 V DC bias) at 183.4 MHz with a rejection of 32 dB and a −20-dB bandwidth of 34 kHz (0.019%). An improved insertion loss of 11 dB at 180 MHz is due to the higher Z_g and resulting higher feed-through current, $i_f(s)$. Similar behavior is observed for the 184.6-MHz mode. The sensitivity of the parallel to series resonance tuning to higher Z_g is revealed in Fig. 4. The degraded rejection with improved insertion loss is as predicted by the model with these particular modes, their motional resistances and associated bias voltages. There is no intrinsic trade-off between rejection and insertion loss with this current cancellation method. Improved insertion loss, achieved with higher Z_g, must be accompanied by lower motional resistance to simultaneously achieve high rejection. In summary, in addition to ferroelectric tuning of the piezoelectric and dielectric constants, Z_g may also be tailored to vary the frequency response.

In conclusion, PZT-on-silicon micromachined resonators showing promise for bandstop filter applications and the associated theory have been introduced. It was shown that currents associated with the parasitic impedances of the electromechanical resonator can be tailored to show either a bandpass or bandstop frequency response. By varying the parasitic resistances and DC bias, one can define the desired frequency response for a single device to either function as a bandstop or bandpass filter. For future devices, the use of low insertion loss series modes with high feed-through, via higher Z_g, will be leveraged to improve the passband loss.

We thank Brian Power and Joel Martin (Army Research Lab) for the device fabrication.

[1]C.-C. Lo, F. Chen, and G. K. Fedder, in Proceedings of the 13th International Conference on Solid-State Sensors, Actuators, and Microsystems, Seoul, South Korea, 5–9 June 2005 (IEEE, New York, 2005), pp. 2074–2077.
[2]J. Wang, Z. Ren, and C. T. -C. Nguyen, IEEE Trans. Ultrason. Ferroelectr. Freq. Control **51**, 1607 (2004).
[3]D. Galayko, A. Kaiser, B. Legrand, L. Buchaillot, C. Combi, and D. Collard, Sens. Actuators, A **126**, 227 (2006).
[4]S. S. Bedair, J. Pulskamp, B. Morgan, and R. Polcawich, in *Proceedings of the PowerMEMS*, Washington, DC, 1–4 December 2009 (TRF, San Diego, California, 2009), pp. 436–438.
[5]G. Piazza, P. L. Stephanou, and A. P. Pisano, J. Microelectromech. Syst. **16**, 319 (2007).
[6]G. K. Ho, R. Abdolvand, A. Sivapurapu, S. Humad, and F. Ayazi, J. Microelectromech. Syst. **17**, 512 (2008).
[7]R. H. Olsson, J. G. Fleming, K. E. Wojciechowski, M. S. Baker, and M. R. Tuck, in *Proceedings of the IEEE Frequency Control Symposium*, Geneva, Switzerland, 29 May-1 June 2007 (IEEE, New York, 2007), pp. 412–419.
[8]D. Jachowski, in IEEE MTT-S International Microwave Symposium Digest, Long Beach, CA, 12–17 June 2005, (IEEE, New York, 2005), pp. 513–516.
[9]I. Reines, S. J. Park, and G. M. Rebeiz, IEEE Trans. Microwave Theory Tech. **58**, 1887 (2010).
[10]H. Chandrahalim, S. A. Bhave, R. Polcawich, J. Pulskamp, D. Judy, R. Kaul, and M. Dubey, Appl. Phys. Lett. **93**, 233504 (2008).
[11]H. Chandrahalim, S. A. Bhave, R.G. Polcawich, J. Pulskamp, D. Judy, R. Kaul, and M. Dubey, *Solid State Sensor, Actuator and Microsystems Workshop*, Hilton Head Island, South Carolina, 2008 pp. 360–363.
[12]R. G. Polcawich and J. F. Pulskamp, "Additive processes for piezoelectric materials: Piezoelectric MEMS," in *MEMS Materials and Processes Handbook*, 1st ed., edited by R. Ghodssi and P. Lin (Springer, New York, 2011), Vol. 3, pp. 273–344.